Electronic Supplementary Information (ESI)

Eco-Friendly Cellulose Nanofibrils with High Surface Charge and Aspect Ratio for Nanopaper Films Having Ultrahigh Toughness and Folding Endurance

Da Zhang,[⊥a] Kexia Jin,[⊥ a] Khak Ho Lim,[b] Suyun Jie,[a] Wenjun Wang,[ab] Xuan Yang*[ab]

[a] State Key Laboratory of Chemical Engineering, Key Laboratory of Biomass Chemical Engineering of Ministry of Education, College of Chemical and Biological Engineering, Zhejiang University, Hangzhou 310027, P.R. China

[b] Institute of Zhejiang University, Quzhou, 324000, P.R. China;

[⊥] *D. Zhang and K. Jin contribute equally*

Table S1 Components, crystallinity and yield of pulp-fiber, MA-CNF, and TEMPO-CNF.

	Lignin (%) [a]	Hemi-cellulose (%) [a, b]	Cellulose (%) [a]	*Crystallinity index* (%) [c]	*yield* (%) [d]
Pulp-fiber	3.0	14.4	82.7	81.7	-
MA-CNFs	4.9	4.2	90.9	70.5	95
TEMPO-CNFs	10.5	10.9	78.6	73.3	80

[a]. The **chemical components** were determined following the standard of National Renewable Energy Laboratory (NREL/TP-510-42618 "Determination of Structural Carbohydrates and Lignin in Biomass Laboratory Analytical Procedure") method.

[b]. Only xylan was detected in the hemicellulose project of all the sample.

[c]. The crystallinity was determined by the X-ray diffraction (XRD, **Fig. S3**), and the **Crystallinity index** (*CrI*) was calculated as follows:

$$CrI = \frac{I_{200}}{I_{200}+I_{am}} \times 100\% \quad (1)$$

where I_{200} is the intensity of 200 peak, I_{am} is the intensity of amorphous peak (intensity minimum between the 200 peak and 110 peak).

[d]. The **yield** represents the ratio of the mass of the final product (CNF) and the mass of the fiber raw material (pulp fiber).

Table S2 Surface group information of MA-CNFs and TEMPO-CNFs.

	σ_{charge} (μmol/g) [a]	ω_{MA} [b]	DS [c]
MA-CNFs	1600(50)	0.192	0.321
TEMPO-CNFs	1150(50)	-	-

[a]. The **charge density** (σ_{charge}, μmol g^{-1}) was calculated by **Fig. S5**.

[b]. The mass fraction of grafted maleic acid group (ω_{MA}) was calculated as follows:

$$\omega_{MA} = \frac{120\times\sigma_{charge}}{1\times10^6} \quad (3)$$

where 120 (g mol^{-1}) is the molecular mass gain from hydroxyl to monoester (C_4HO_3Na).

[c]. The degree of substitution (*DS*) on the MA-CNFs was calculated as follows:

$$DS = \frac{162\times\sigma_{charge}}{(1-\omega_{MA})\times10^6} \quad (4)$$

where 162 (g mol^{-1}) is the molecular mass of the glucose units in the cellulose ($C_6H_{10}O_5$).

Table S3 Optimization of the reaction conditions for esterification of maleic anhydride. [a]

	A: Reaction Temperature (°C)	B: Water Content (wt.%) [b]	Response: IR carbonyl [c]
1	60	0	0.229(0.012)
2	60	20	0.258(0.008)
3	95	0	0.291(0.010)
4	95	20	0.334(0.001)

[a]. Two variables, **(A) reaction temperature** and **(B) water content**, were considered. Other reaction conditions remained unchanged. **IR carbonyl** was used as the response value. All samples were tested three times and the average and standard deviation were reported. Esterification product were fully washed with deionized water without alkali treatment. Typical IR spectra of MA esterified pulp fiber was shown in **Fig. S6** for reference.

[b]. **Water content** is the mass fraction (based on the dry weight of pulp fiber) of added water.

[c]. **IR carbonyl** is defined as the ratio of IR absorbance at 1720 cm^{-1} (C=O) and IR absorbance at 3334 cm^{-1} (-OH, as internal standard).

Table S4 Mechanical properties of different pulp-paper-based CNF nanopaper films.

Num.	Reference	Pretreatment	Tensile Strength (MPa)	Young's Modulus (GPa)	Strain at failure (%)	Toughness (MJ/m^3)
1	This work	MA	200	8.7	16.4	12.2
2	This work	H-MA	189	10.5	15.2	11.8
3	This work	De-MA	191	12.0	8.1	6.0
4	REF1	N/A	132	5.7	8.2	9.4
5	REF1	N/A	131.1	9.0	2	2.4
6	REF2	N/A	96.3	3.4	4.9	7.5
7	REF3	N/A	89	9	0.9	0.9
8	REF4	PAA	320	21	9.8	4.8
9	REF5	TEMPO	275	-	11.7	8.5
10	REF6	TEMPO	237	14.9	8.1	5.0
11	REF7	TEMPO	140	4.4	8.6	7.8
12	REF8	TEMPO	210	11.7	4.2	3.2
13	REF9	TEMPO	218	10.3	10.7	7.5
14	REF10	TEMPO	105	-	1.9	2.1
15	This work	TEMPO	216	14.7	4.4	3.1
16	REF11	Enzymatic	181	10.4	9.1	7.4

Num.	Reference	Pretreatment	Tensile Strength (MPa)	Young's Modulus (GPa)	Strain at failure (%)	Toughness (MJ/m^3)
17	REF12	Enzymatic	218	13.8	14.1	9.7
18	REF12	Enzymatic	193	15.4	6.4	4.9
19	REF13	Enzymatic	196	10.4	6.5	5.0
20	REF14	Enzymatic	243	14.9	9.2	6.0
21	REF15	Enzymatic	175	9.9	10.3	8.5
22	REF16	Carboxymethylation	198	-	11.0	8.2
23	REF11	Carboxymethylation	214	13.2	15.1	10.1
-	REF17[a]	N/A	1015	60.2	≈3	15.2
-	REF18[b]	TEMPO	380	46	1.5	-
-	REF19[c]	TEMPO	185	10.3	5.3	-
-	REF19[c]	TEMPO	428	24.6	2.5	-
-	REF19[c]	TEMPO	397	33.3	1.8	-

[a]. The nanopaper film reported in REF17 was oriented films.

[b]. The nanopaper film reported in REF18 was oriented films with a draw ratio of 1.3.

[c]. The nanopaper films reported in REF19 were oriented films with a draw ratio of 1, 1.4, 1.6, separately.

Table S5 Mechanical property data of pulp fiber films, standard deviations are reported.

	Tensile Strength (MPa)	Young's Modulus (GPa)	Strain at failure (%)	Toughness (MJ/m^3)
Pulp-fiber	45 (3)	4.9 (0.8)	1.9 (0.1)	0.5 (0.1)

Table S6 The porosity of different paper films.

	porosity (%)[a]
Pulp-fiber	34
MA-CNF	4
TEMPO-CNF	4
H-MA-CNF	11
De-MA-CNF	13

[a]. The *porosity* was calculated as follows:

$$porosity = (1 - \frac{m}{\rho \times \mu \times S}) \times 100\% \quad (5)$$

where m is the mass of paper film (g), ρ is the density of paper films (1.55 g cm^{-3}), μ is the thickness of paper film (cm), S is the area of paper film (cm^2).

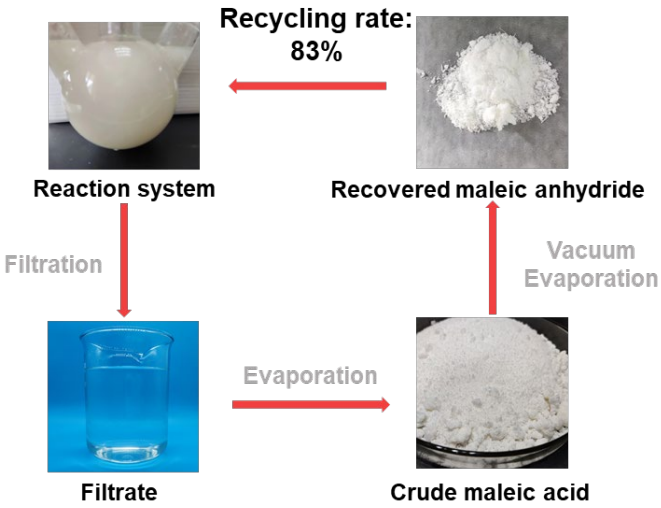

Fig. S1 The recycling route of maleic anhydride.

The recycling of maleic anhydride includes three steps: 1) obtain maleic acid filtrate through filtration and separation of fibers, 2) evaporate the filtrate at 80-120ºC to concentrate the maleic acid, 3) dehydrate the maleic acid to obtain maleic anhydride using vacuum evaporation at 100-160 ºC. Note that the recycling rate is calculated by the ratio of the mass of recycled MA (81.7 g) and the mass of unreacted MA (98.6 g). The liquid-state ^{1}H NMR spectrum of pure maleic anhydride and recycled maleic anhydride is shown in **Fig. S4**.

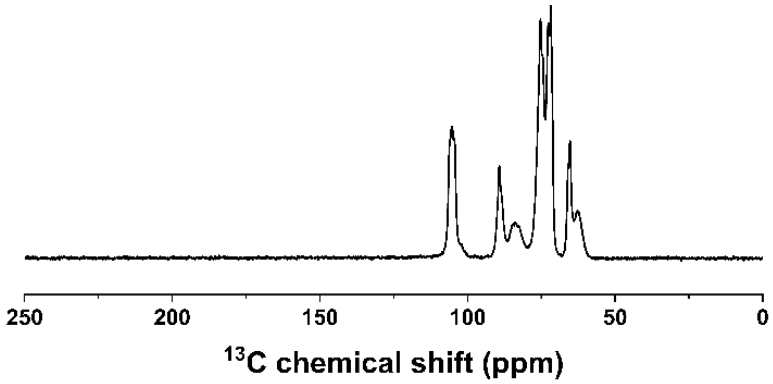

Fig. S2 Solid-state ^{13}C NMR spectrum of pulp-fiber.

Note that the solid-state ^{13}C NMR of both pulp fibers and MA-CNFs was measured on an Avance neo 600WB (Bruker, Germany) equipment by using total sideband suppression (TOSS) sequence. About 150 mg of freeze-dried sample of ^{13}C NMR was soaked in the deionized water for at least half a day. The measurement was at ambient temperature with a spinning rate of 10 kHz, a recycle delay of 5s and 2000 scans. Chemical shift was referenced by Adamantane at 38.5 ppm.

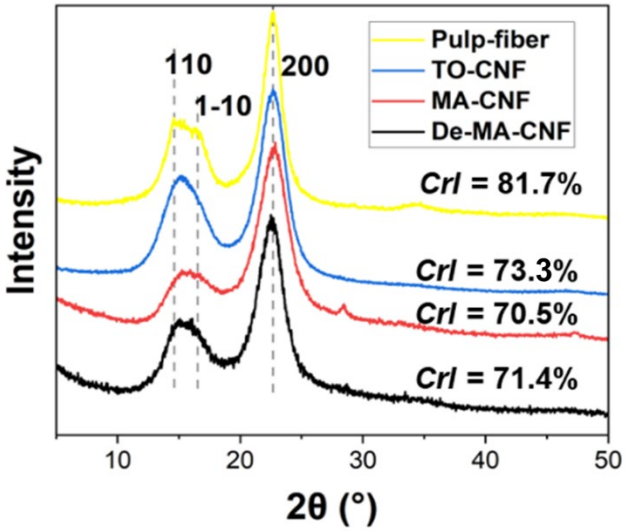

Fig. S3 XRD of pulp-fiber, MA-CNFs, TO-CNFs, and De-MA-CNFs.

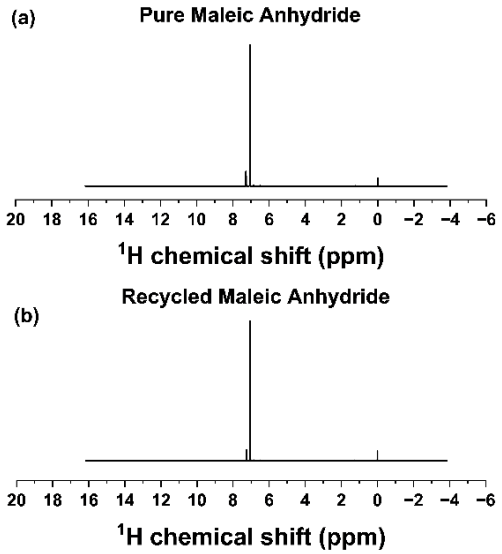

Fig. S4 Liquid-state ^{1}H NMR spectrum of pure maleic anhydride (a) and recycled maleic anhydride (b).

Note that maleic anhydride is dissolved in deuterated chloroform ($CDCl_3$, 7.28 ppm shift) and the chemical shift is calibrated using tetramethyl silane (TMS, 0 ppm shift). The 7.06 ppm shift peak belongs to the 2',3'-H of maleic anhydride. The peaks of maleic acid at 6.285 ppm and 11 ppm are not found in the recycled maleic anhydride, indicating that the recycled maleic anhydride is of high purity.

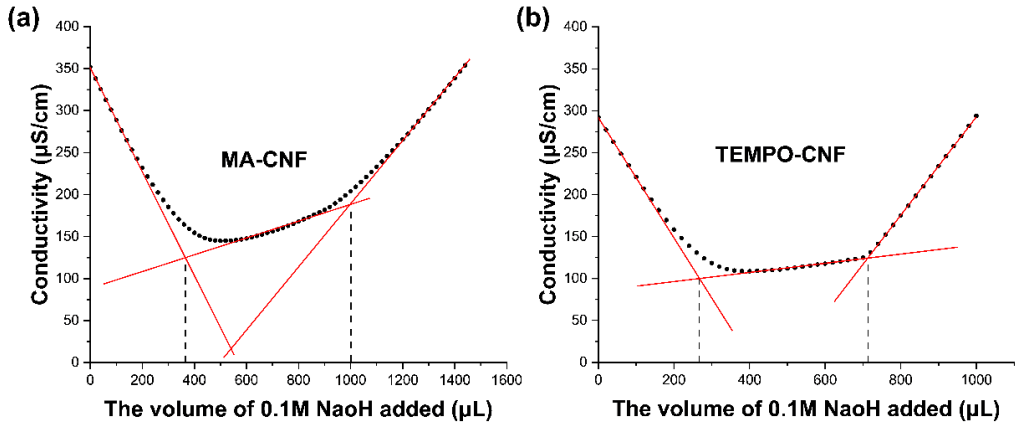

Fig. S5 Conductometric titration curve to determine the surface carboxylate content of MA-CNFs (a) and TEMPO-CNFs (b).

Conductometric titration was used to determine the **surface carboxylate content** of MA-CNFs and TEMPO-CNFs. Before the titration, 0.04 g of CNFs (with -COONa) was dispersed in deionized water and treated by cationic resin for over 7 days for thoroughly protonation. HCl solution was added before the titration. 0.1M of NaOH was used for the titration. The plateau between two turning points in the titration curve (**Fig. S5**) was used to calculate the **carboxylate content** of CNFs. The measurement was conducted in triplicate.

The surface **charge density** (σ_{charge}, μmol g^{-1}) of CNFs is considered equal to the **surface carboxylate content** and was calculated by the following equation:

$$\sigma_{charge} = \frac{V_{NaOH} \times c_{NaOH}}{m_{CNF}} \quad (2)$$

where V_{NaOH} is the volume of consumed NaOH solution (mL), c_{NaOH} is the molar concentration of NaOH solution (100 μmol mL^{-1}), m_{CNF} is the mass of CNF used during the titration (0.04 g).

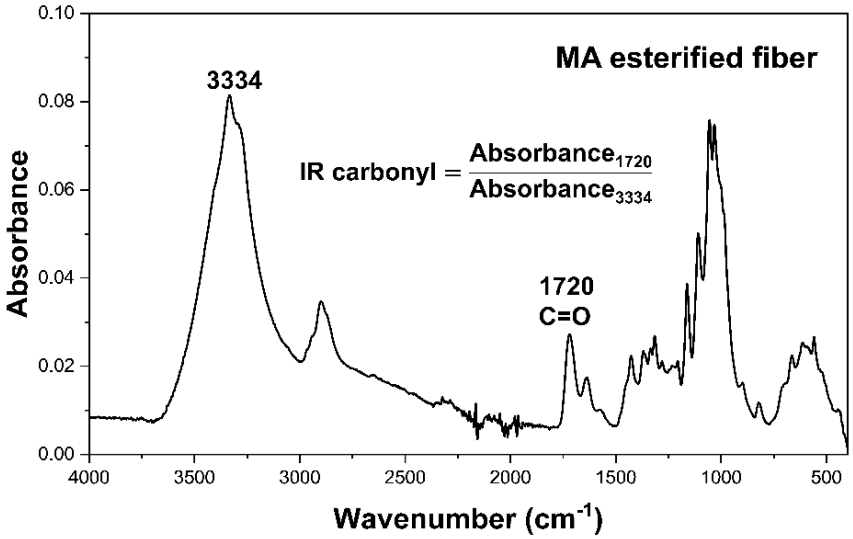

Fig. S6 The typical IR spectra of maleic anhydride esterified pulp fiber, the esterification variable is in 95° C and 20 wt.% water added.

Note that the 1720 cm^{-1} peak on the IR spectrum belongs to the carbonyl group of the grafted maleic acid ester, which indicates that MA reaction is esterification reaction. The 1640 cm^{-1} peak on the infrared spectrum belongs to the C=C group. The IR spectrum of the raw material is in **Fig.S7** for reference.

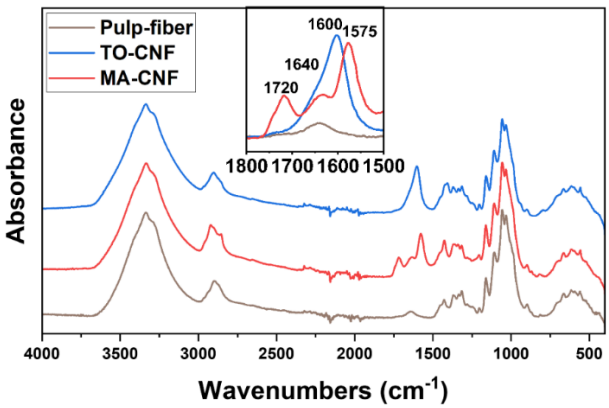

Fig. S7 The IR spectra of raw materials pulp fiber, MA-CNF, TEMPO-CNF, in which the 1800-1500cm^{-1} region is amplified

Note that the 1575 cm^{-1} peak (MA-CNF) and 1600 cm^{-1} peak (TEMPO-CNF) on the infrared spectrum both belong to the carboxyl group (in Na form), which indicates surface charge comes from carboxyl group. The red shift of the carboxyl peak of MA-CNF is attributed to the conjugation of C=C in the grafted maleic acid. The 1720 cm^{-1} peak (MA-CNF) on the infrared spectrum belongs to the ester group, which indicates that MA reaction is esterification reaction.

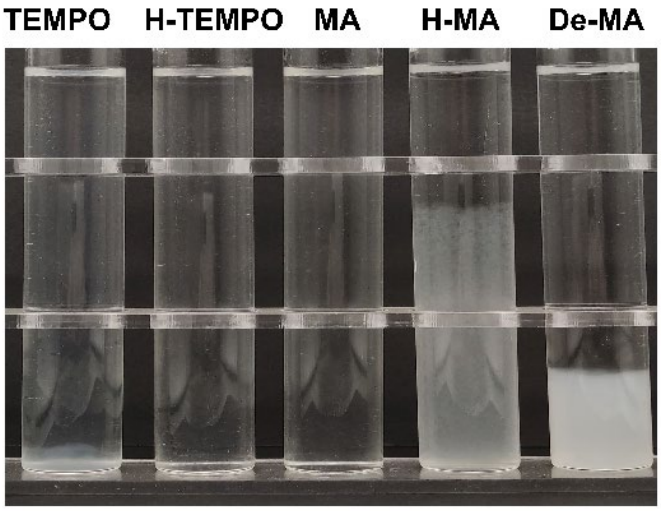

Fig. S8 Photos of 0.2 wt.% TEMPO-CNF, H-TEMPO-CNF, MA-CNF, H-MA-CNF, and De-MA-CNF dispersion.

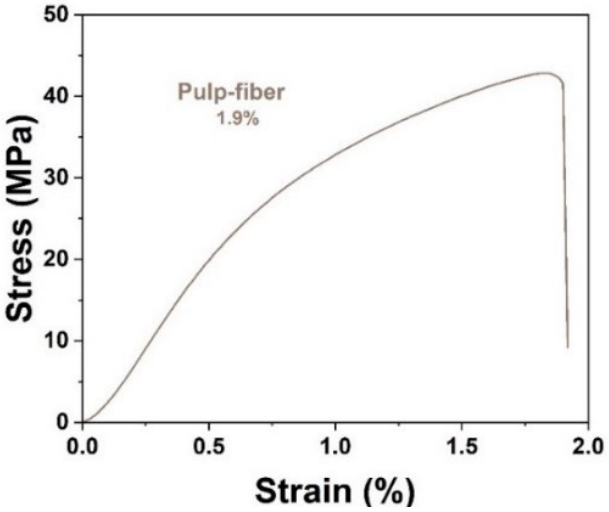

Fig. S9 Stress-strain curve of pulp paper films.

Note that the pulp fiber film is prepared from the same weight pulp fiber through the same preparation process with nanopaper films.

Reference

1 M. Farooq, T. Zou, G. Riviere, M. H. Sipponen and M. Österberg, Biomacromolecules, 2019, 20, 693–704.

2 F. Chen, W. Xiang, D. Sawada, L. Bai, M. Hummel, H. Sixta and T. Budtova, ACS Nano, 2020, 14, 11150–11159.

3 J. Lucenius, K. Parikka and M. Österberg, React. Funct. Polym., 2014, 85, 167–174.

4 X. Yang, M. S. Reid, P. Olsén and L. A. Berglund, ACS Nano, 2020, 14, 724–735.

5 H. Zhu, S. Zhu, Z. Jia, S. Parvinian, Y. Li, O. Vaaland, L. Hu and T. Li, Proc. Natl. Acad. Sci., 2015, 112, 8971–8976.

6 M. Shimizu, T. Saito and A. Isogai, J. Membr. Sci., 2016, 500, 1–7.

7 Y. Liu, S.-H. Yu and L. Bergström, Adv. Funct. Mater., 2018, 28, 1703277.

8 C.-N. Wu, Q. Yang, M. Takeuchi, T. Saito and A. Isogai, Nanoscale, 2014, 6, 392–399.

9 T. Kurihara and A. Isogai, Cellulose, 2015, 22, 2607–2617.

10 Z. Fang, H. Zhu, Y. Yuan, D. Ha, S. Zhu, C. Preston, Q. Chen, Y. Li, X. Han, S. Lee, G. Chen, T. Li, J. Munday, J. Huang and L. Hu, Nano Lett., 2014, 14, 765–773.

11 M. Henriksson, L. A. Berglund, P. Isaksson, T. Lindström and T. Nishino, Biomacromolecules, 2008, 9, 1579–1585.

12 K. Prakobna, V. Kisonen, C. Xu and L. A. Berglund, J. Mater. Sci., 2015, 50, 7413–7423.

13 R. Mao, N. Meng, W. Tu and T. Peijs, Cellulose, 2017, 24, 4627–4639.

14 F. Ansari, M. Skrifvars and L. Berglund, Compos. Sci. Technol., 2015, 117, 298–306.

15 H. Sehaqui, Q. Zhou and L. A. Berglund, Soft Matter, 2011, 7, 7342–7350.

16 J. Zhou, Z. Fang, J. Cui, X. Zhang, Y. Qian, W. Liu, D. Yang and X. Qiu, Carbohydr. Polym., 2021, 259, 117759.

17 Z. Fang, B. Li, Y. Liu, J. Zhu, G. Li, G. Hou, J. Zhou and X. Qiu, Matter, 2020, 2, 1000–1014.

18 W. Gindl-Altmutter, S. Veigel, M. Obersriebnig, C. Tippelreither and J. Keckes, in Functional Materials from Renewable Sources, American Chemical Society, 2012, vol. 1107, pp. 3–16.

19 H. Sehaqui, N. Ezekiel Mushi, S. Morimune, M. Salajkova, T. Nishino and L. A. Berglund, ACS Appl. Mater. Interfaces, 2012, 4, 1043–1049.